Magn Reson Med Sci 2019; 18; 119–125
doi:10.2463/mrms.mp.2018-0011
Published Online: July 13, 2018

MAJOR PAPER

How to Improve the Conspicuity of Breast Tumors on Computed High *b*-value Diffusion-weighted Imaging

Takayuki Tamura[1*], Miyuki Takasu[2], Toru Higaki[2,3], Kazushi Yokomachi[1], Yuji Akiyama[1], Hiroomi Sumida[1], Yasushi Nagata[1,3], and Kazuo Awai[2,3]

Purpose: The aim of this study was to compare the tumor conspicuity on actual measured diffusion-weighted images (aDWIs) and computed DWI (cDWI) of human breast tumors and to examine, by use of a phantom, whether cDWI improves their conspicuity.

Materials and Methods: We acquired DWIs (*b*-value 0, 700, 1400, 2100, 2800, and 3500 s/mm^2) of 148 women with breast tumors. cDWIs with *b*-values of 1400, 2100, 2800, and 3500 s/mm^2 were calculated from aDWI scans where b = 0 and 700 s/mm^2; the tumor signal-to-noise ratio (SNR) was compared at each *b*-value. We also subjected a phantom harboring a breast tumor and mammary glands to DWI. For reference we used two models. The model with b = 0, 1000, 1500, 2000, 2500, and 3000 s/mm^2 was our multiple *b*-value model. In the single *b*-value model, we applied b = 0 and 1000 s/mm^2 and changed the number of excitations (NEX). cDWIs were generated at b = 0 and 1000 and used to compare the SNR, the contrast ratio (CR), and the contrast-to-noise ratio (CNR).

Results: In the phantom study, the CNR of cDWI generated from high SNR images obtained at lower *b*-values and a high NEX was outperformed aDWI. However, the CR and CNR on cDWI obtained using the same scanning parameters were inferior to aDWI scans. Similarly, in the clinical study, breast tumor conspicuity was worse on high *b*-value cDWIs than aDWIs.

Conclusion: To improve tumor conspicuity on cDWI, the quality of the source images must be improved. It may easily cause inferior conspicuity to aDWIs if high *b*-value cDWIs were generated from insufficient SNR images.

Keywords: *breast tumor, computed diffusion-weighted image, multi-exponential diffusion-weighted image decay*

Introduction

Diffusion-weighted image (DWI) is of clinical utility for the diagnosis of breast tumors[1–7] and although many institutes adopt DWI with *b*-values below 1000 s/mm^2,[8,9] DWI with higher *b*-values is diagnostically useful.[10–13] However, its diagnostic capability may be limited by a lower signal-to-noise ratio (SNR) which decreases tumor conspicuity.[12,13]

Computed DWI (cDWI) is a mathematical technique that can generate virtual DWI with higher *b*-values from DWI with two arbitrary lower *b*-values.[14] It not only avoids the SNR decrease and scan time prolongation associated with the direct acquisition of high *b*-value images but it may also help to abate image distortion.[14–18]

While some study[17,18] found that cDWI was advantageous for the detection of tumors on whole-body and breast scans, lesion conspicuity was compared only on actual DWI (aDWI) scans and cDWIs acquired with different *b*-values. To ascertain the true validity of cDWI, aDWI and cDWI obtained at identical parameters or scan time should be compared.

We compared the conspicuity of human breast tumors on high *b*-value aDWIs and cDWIs performed with identical scanning parameters. We also prepared a multi-exponential DWI signal decay phantom to determine whether breast tumor conspicuity can be improved on cDWIs.

[1]Department of Radiology, Hiroshima University Hospital, 1-2-3 Kasumi, Minami-ku, Hiroshima, Hiroshima 734-8551, Japan
[2]Department of Diagnostic Radiology, Hiroshima University, Hiroshima, Japan
[3]Graduate School of Biomedical & Health Sciences, Hiroshima University, Hiroshima, Japan

*Corresponding author, Phone: +81-82-257-5555, Fax: +81-82-257-5555, E-mail: tktamura@hiroshima-u.ac.jp

Received: January 24, 2018 | Accepted: May 23, 2018

Materials and Methods

Study population

Our retrospective study was approved by our institutional review board. Between November 2009 and July 2011, 192 women (201 breast tumors) underwent breast MRI for further evaluation of mammography or ultrasound findings. We excluded 44 patients because MRI failed to detect tumors. Consequently, 148 women (154 breast tumors) were included in this study; their median age was 59.0 years (range = 21−86 years), the median tumor size was 20.0 mm (range 4–60 mm).

In all patients, breast tumors were surgically rejected and the final diagnosis based on histopathological findings that identified 119 invasive and 15 non-invasive ductal carcinomas, eight mucinous carcinomas, four invasive lobular carcinomas, two phyllodes tumors (one was benign and the other one was borderline), two malignant lymphomas, two ductal adenomas, one medullary carcinoma, one squamous cell carcinoma.

MR image acquisition

Magnetic resonance imaging studies, including DWI at multiple *b*-values were performed on 1.5T superconducting scanner (Gyroscan Achieva R.2.6; Philips Medical Systems, Best, The Netherlands) using a 7-channel sensitivity encoding (SENSE) breast coil. With the patients in prone position, axial DWI scans were obtained using a spin-echo-type single shot echo planar imaging (EPI) technique. The EPI sequence incorporated a spectral-selective inversion recovery (SPAIR) radio frequency pulse for effective fat suppression. The DWI parameters were TR 5600 ms, TE 99 ms, matrix 128 × 114 (256 reconstruction), FOV 280 mm, thickness 4 mm, slice 24, half-scan factor 0.6, SENSE factor 2.0 and number of excitation (NEX) 3 (Average high *b*-value function was not used). We applied six diffusion *b*-values (0 to maximum 3500 s/mm^2 in 700 s/mm^2 increments). The multiple *b*-value DWI scan time was 4 min 40 s. After the DWI we acquired axial images of both breasts using a fast-spin-echo T_2-weighted (T_2W) sequence with fat-suppuration, a T_1-weighted (T_1W) gradient echo sequence, and a dynamic contrast enhanced sequence after the intravenous injection of gadolinium contrast medium (0.2 ml/kg delivered at 2 ml/s).

Generation of cDWI

Computed DWIs were generated using a plug-in tool developed in-house for ImageJ (http://rsbweb.nih.gov/ij/, National Institute of Health, Bethesda, MD, USA), freely available on the Digital Imaging and COmmunications in Medicine (DICOM) viewer cDWI scans were calculated with mono-exponential equation from aDWI scans (b = 0 and 700 s/mm^2):

$$S_b = S_1 \exp(-\Delta b \cdot D) \quad (1)$$

$$D = \ln\left\{\frac{(S_1 - S_2)}{(b_1 - b_2)}\right\} \quad (2)$$

where S_1 and S_2 is the signal intensity (SI) at two arbitrary *b*-values ($b_1 < b_2$ s/mm^2), Δb is a difference between b_1 and b_2 ($b_1 < b_2$) and D is the apparent diffusion coefficient (ADC).[14]

Comparison of lesion conspicuity on aDWI and cDWI scans

We generated cDWIs and aDWIs with b = 1400, 2100, 2800, and 3500 s/mm^2 (Fig. 1a). We placed ROI that did not include normal tissue in the target tumor. The ROIs was identified by comparing images obtained in the dynamic study (Fig. 1b and 1c) and was placed on the same site on aDWIs and cDWIs. The SNRs was calculated by dividing the SI by standard deviation (SD) of the ROIs and compared on aDWIs and cDWIs obtained at each *b*-value. We also calculated the SNR rate by dividing the SNR on cDWIs by the SNR on aDWIs and recorded it for each *b*-value. We tested the statistical significance of differences using Wilcoxon single rank test with a commercial program (JMP v.13.0, SAS Institute Inc., Cary, NC, USA). Differences of $P < 0.01$ were considered significant.

Phantom study

According to the previous study,[19] the signal decay of most breast tumors is bi-exponential while that of normal mammary glands is mono-exponential vis-à-vis the function of *b*-value.

We used the partial volume effect to create a phantom that mimicking breast tumor with combination fast and slow diffusion components. Saline was the fast and gelatin gel (50 wt%) the slow component. The slow component was placed in the lower half of 10-mm diameter acrylic tube, the upper half was then filled with saline. We obtained DWIs at different *b*-values at the interface of the gel and saline where bi-exponential signal decay was expected (Fig. 2).

To create the mono-exponential decay phantom mimicking background of normal breast, we used polyvinyl alcohol (PVA) gel (8 wt%). We added 0.2 mmol/l $MnCl_2$ for shortening of T_2 value of PVA gel to obtain an initial SI that was the same as on b = 0 images of normal breast (Fig. 2).

We used a 3T scanner (Achieva; Philips Medical Systems, Best, The Netherlands) and a 16-channel phased-array head coil for signal reception. DWI was performed using single-shot EPI with SPAIR; the scanning parameters were TR 5600 ms, matrix 128 × 116 (256 reconstruction), FOV 100 mm, slice thickness 10 mm, half-scan factor 0.65, SENSE factor 2.0. For reference we again used two models; the multiple *b*-value series applied b = 0, 1000, 1500, 2000, 2500 and 3000 s/mm^2. The single *b*-value series involved b = 0 and 1000 s/mm^2. TE varied according to the maximum *b*-value. TE of multiple *b*-value series and single *b*-value series was 103 and 81 ms, respectively. With the single *b*-value series we also used three NEX (i.e. 2, 4, and 8) (Average high *b*-value

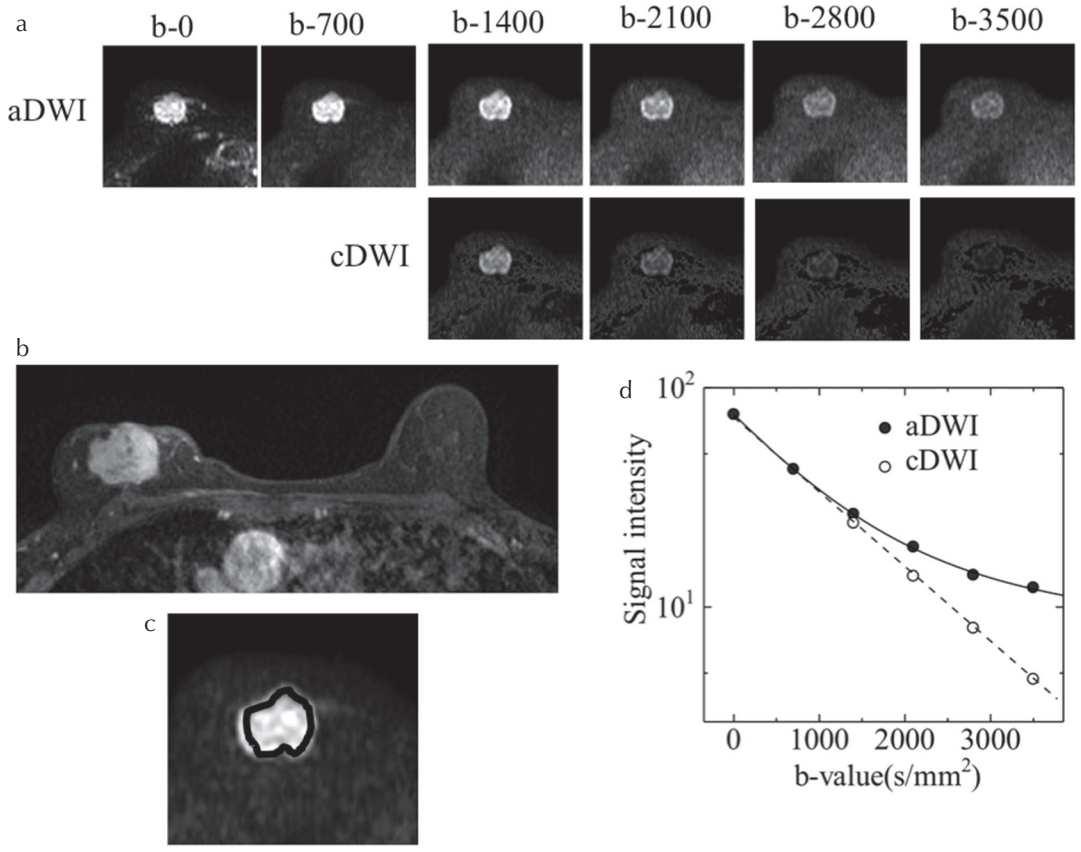

Fig. 1 Actual measured diffusion-weighted image (aDWI) and computed DWI (cDWI) of a 76-year-old woman with invasive ductal carcinoma. (**a**) Upper: aDWI, lower: cDWI (b = 0 and 700 s/mm^2). (**b**) 3D T_1-weighted fast gradient-echo image obtained after the administration of contrast medium. (**c** and **d**) ROI position (**c**) and signal decay of aDWI and cDWI (**d**).

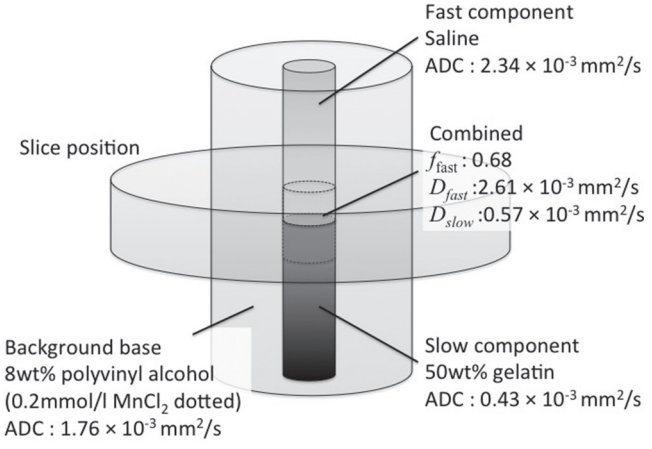

Fig. 2 Schema of our phantom mimicking a breast tumor and normal mammary gland. The bi-exponential decay on diffusion-weighted images (DWIs) was constructed by scanning the interface between the fast and the slow component using the partial volume effect. ADC, apparent diffusion coefficient.

function was not used). The scan time of multiple b-value series was 3 min 4 s and single b-value series of NEX 2, 4, 8 were 50 s, 1 min 34 s and 3 min 4 s, respectively.

Actual DWI scans were displayed using image J. cDWI scans were generated with a plug-in tool from b-value combination between b = 0 and 1000 s/mm^2 of each series. The ROIs were set in the mass and background base adjacent to the mass and their SI and SD were recorded. We then calculated and compared the SNR of mass and the background base, the tumor: background contrast (CR) and the contrast-to-noise ratio (CNR). SNR, CR and CNR were calculated using the formula:

$$\mathrm{SNR} = \frac{\mathrm{SI_{ROI}}}{\mathrm{SD_{ROI}}} \quad (3)$$

$$\mathrm{CR} = \frac{\left(\mathrm{SI_{mass}} - \mathrm{SI_{BG}}\right)}{\left(\mathrm{SI_{mass}} + \mathrm{SI_{BG}}\right)} \quad (4)$$

$$\mathrm{CNR} = \frac{\left(\mathrm{SI_{mass}} - \mathrm{SI_{BG}}\right)}{\sqrt{\frac{\mathrm{SD^2_{mass}} + \mathrm{SD^2_{BG}}}{2}}} \quad (5)$$

Results

Clinical study

The mean SNR was significantly lower on cDWI- than aDWI scans ($P < 0.001$, data not shown). The SNR rate between aDWI and cDWI is shown in Fig. 3. The SNR rate decreased significantly as the b-value increased ($P < 0.001$). Figure 1 illustrates a representative patient with invasive ductal carcinoma. The SI was lower on cDWI- than aDWI scans (Fig. 1d) and the tumor became gradually less conspicuous; it was not visualized at b = 3500 s/mm^2 (Fig. 1a). Under identical scanning parameters, tumor detection was more difficult on cDWI than aDWI scans.

Phantom study

Figure 4 presents aDWI and cDWI scans of our phantom, and Fig. 5 the DWI signal decay of each component. The ADC of the fast component (saline) was 2.34×10^{-3} mm^2/s; it was 0.43×10^{-3} mm^2/s for the slow component (50 wt% gelatin gel). The DWI signal decay of both was clearly mono-exponential. Application of the partial volume effect showed that the signal decay of the slice at the interface between the two components was clearly bi-exponential (f_{fast}: 0.62, f_{slow}: 0.38, D_{fast}: 2.6×10^{-3} mm^2/s, D_{slow}: 0.57×10^{-3} mm^2/s) (Fig. 5c). The signal decay in the background base mimicking normal breast tissue was mono-exponential with the function of the *b*-value until it reached the background noise level (Fig. 5d).

Comparison of the SNR on multiple *b*-value series aDWI and cDWIs obtained at b = 0 and 1000 s/mm^2 revealed that the SNR of the background was significantly higher on cDWIs than aDWIs at each applied *b*-value. As shown in Fig. 6a, the SNR of the background was higher on single *b*-value series cDWIs with a short TE than on multiple *b*-value series cDWIs and increased as NEX increased. On the other hand, the SNR of the bi-exponential tumor phantom was lower on multiple *b*-value series cDWIs than on aDWIs. It was higher on single- than multiple *b*-value series and cDWI performed at NEX = 4 outperformed aDWI at *b*-values of 1500, 2500, and 3000 s/mm^2. However, at NEX = 8, the SNR of tumors was lower than at NEX = 4; at each applied *b*-value it was almost the same as or slight lower than on aDWIs (Fig. 6b).

On aDWI scans, the tumor: background CR increased with the *b*-value until it reached a plateau; on cDWIs the CR increased linearly with the *b*-value (Fig. 6c). Comparison of the CR showed that cDWIs were inferior to aDWIs at each *b*-value; the CR of cDWI increased as the SNR on source images increased but it did not exceed the CR of aDWIs except at b = 3000 s/mm^2 of the single *b*-value series (Fig. 6c). The CNR on multiple *b*-value series cDWI scans was inferior to the CNR on aDWIs at each *b*-value applied; it was almost the same on single *b*-value series cDWIs at NEX = 2 and on aDWIs. cDWI with NEX = 4 and 8 outperformed aDWI (Fig. 6d).

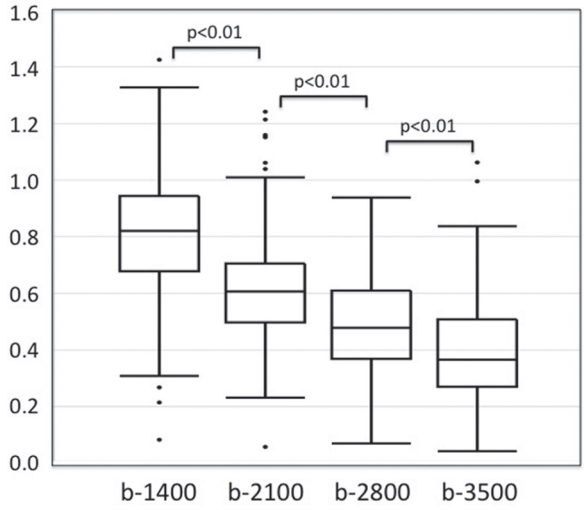

Fig. 3 Comparison of the signal-to-noise ratio (SNR) on computed diffusion-weighted images (cDWIs) and actual measured DWIs (aDWIs) obtained at different *b*-values. The SNR rate was calculated by dividing the SNR on cDWIs by the SNR on aDWIs.

Discussion

Our clinical study showed that, under identical scanning parameters, the conspicuity of breast tumors on high *b*-value

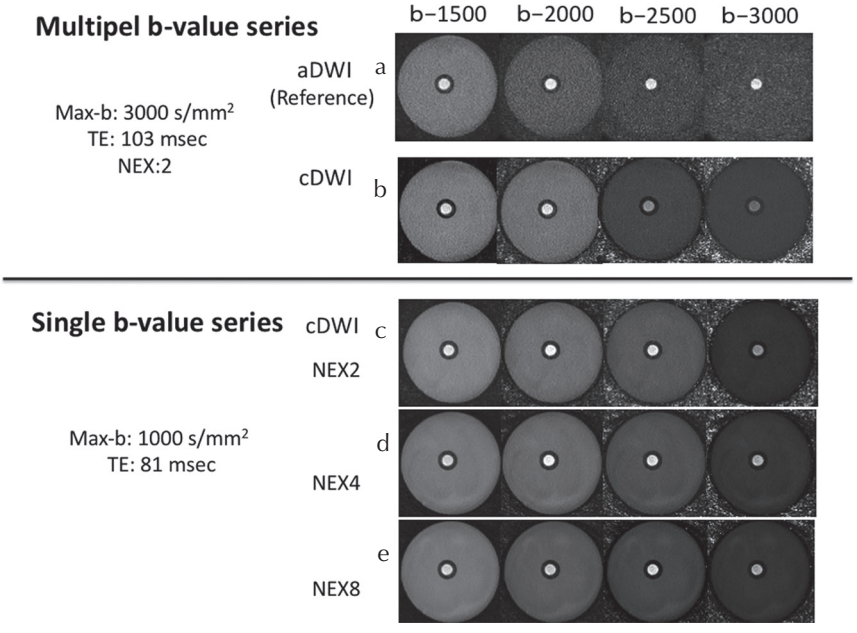

Fig. 4 Phantom study – diffusion-weighted image (DWI). (**a**) Actual measured multiple *b*-value DWI series. (**b**) High *b*-value cDWI (b = 0 and 1000 s/mm^2). (**c**–**e**) Single *b*-value series. TE is shortened and the number of excitations (NEX) is 2, 4, and 8.

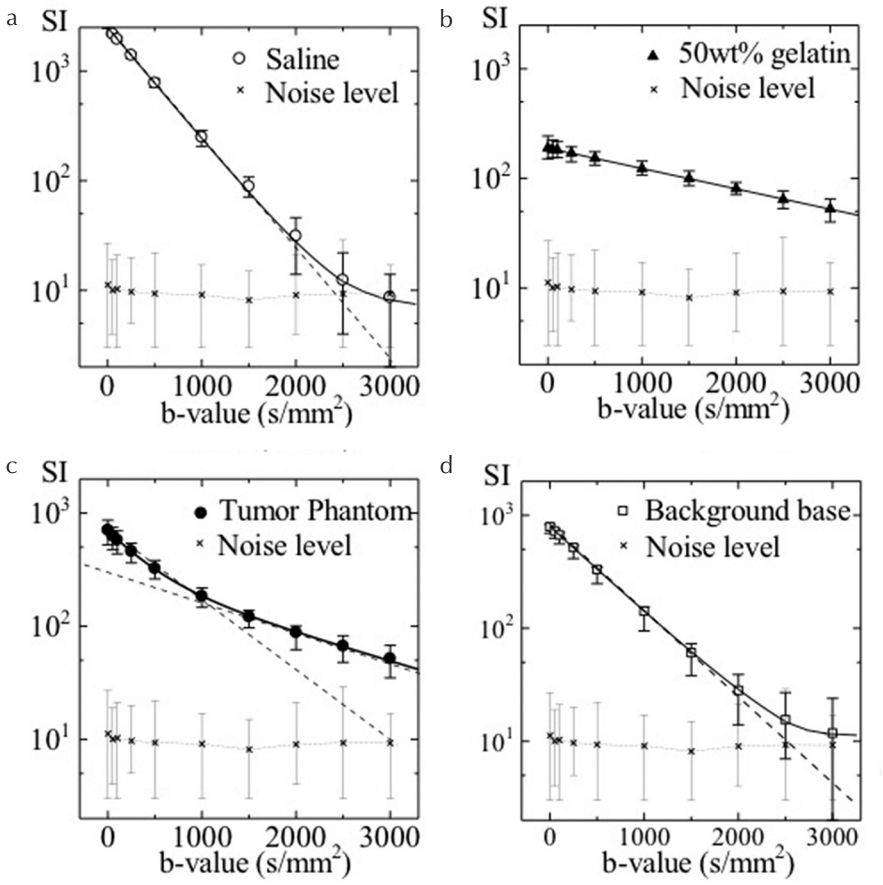

Fig. 5 Graph showing the signal decay of the fast (**a**) and the slow component (**b**) on actual measured diffusion-weighted image (aDWI). The tumor phantom is presented in (**c**) and the background in (**d**).

cDWI scans was inferior to aDWI (Fig. 3). The SI of tumors was lower on cDWIs than on aDWIs because cDWI fit the tumor signal subject to multi-exponential decay to the mono-exponential function (Fig. 1d). Consequently, the underestimation on cDWIs increased with the *b*-value (Fig. 3).

Multiple *b*-value DWI involves long scan times and the use of higher *b*-values prolongs the motion proving gradient application time and the echo time, resulting in a decrease in SI. This complicates tumor detection because the SNR on DWI scans is inherently low. With cDWI, on the other hand, the scan time and the echo time can be shortened. This facilitates the acquisition of DWI scans with arbitrary *b*-values while maintaining the SNR.[14–18] Our clinical study showed that the conspicuity of breast tumors was inferior on cDWIs compared to aDWIs performed with the same imaging parameters. Therefore, we performed phantom experiments in which we simulated the signal attenuation of breast tumors and of the background normal mammary gland to demonstrate the superiority of tumor conspicuity on cDWIs.

First we acquired DWI scans at multiple *b*-values (0, 1000, 1500, 2000, 2500, and 3000 s/mm^2) as reference (multiple *b*-value series, Fig. 4). The reference images were comprised of a series of high *b*-value images. Then, we generated cDWIs from $b = 0$ and 1000 s/mm^2 scans of the same series. At all *b*-values, the SNR of the background was markedly higher on cDWIs than aDWIs (Fig. 6a). However, the tumor SNR was lower on cDWIs than aDWIs (Fig. 6b). The noise level of computed high *b*-value DWI was kept low comparable with low *b*-value source images. The SI of mono-exponential decay materials (e.g. background base) was estimated to be of the same level as on aDWIs, however, the SI of bi-exponential decay materials (e.g. tumor) was underestimated (Fig. 1d). The estimated SI and SNR are lower when the signal decay does not following the mono-exponential theory. Consequently, the tumor: background CR and CNRs are lower than on high *b*-value aDWIs, an observation that supports the findings of our clinical study.

We then created a diffusion model that applied low *b*-values and short TEs to obtain DWI scans with a high SNR (low *b*-value series, Fig. 4). We expected that such high-SNR source images would contribute to an SNR increase on cDWIs. We used *b*-values up to 1000 s/mm^2 to shorten TE and succeeded in decreasing it to 81 ms; at the same time, the SNR of $b = 1000$ s/mm^2 images was increased by 20% (data not shown). Furthermore, the scan time was shortened by approximately 70% when the *b*-value of DWI scans was not higher than 1000 s/mm^2. We obtained cDWIs ($b = 1500$–3000) by using $b = 0$ and 1000 s/mm^2 scans of the single *b*-value series and compared the SNR on the cDWIs with the SNR on aDWI reference scans. At all applied *b*-values, the

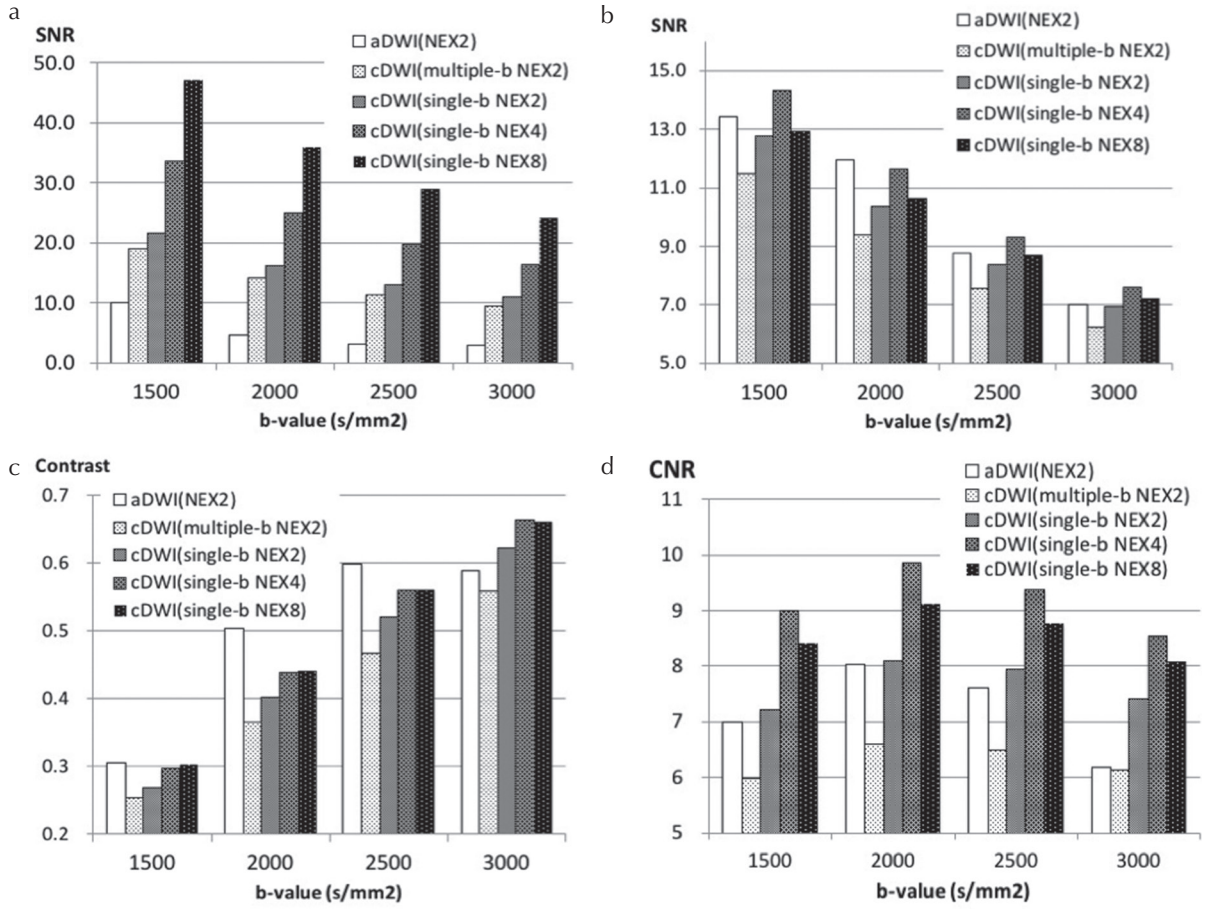

Fig. 6 Comparison of the signal-to-noise ratio (SNR) of the background (**a**) and the tumor phantom (**b**) and comparison of the contrast (**c**) and the contrast-to-noise ratio (CNR) (**d**) on images of the tumor phantom and the background. aDWI, actual measured diffusion-weighted image; cDWI, computed diffusion-weighted image.

SNR of the background at NEX = 2 was twice as great as on aDWIs. When we used the "saved" time to increase NEX from 2 to 4 and to 8, the SNR of the background tripled and quadrupled. The mono-exponentially decaying sample (i.e. the background base) exhibited a markedly high SNR (Fig. 6a) while at each high *b*-value, the SNR of the tumor phantom, which showed bi-exponential decay, was almost the same as on aDWIs (Fig. 6b). This finding is explicable by the observation that the SI of multi-exponentially decaying material was estimated to be lower than the SI on aDWIs, while the noise level remained low.

Comparison of the CNR of single *b*-value series revealed that cDWIs with short TE and NEX 2 outperformed aDWI scans. Furthermore, when NEX was increased, cDWI greatly outperformed aDWI (Fig. 6d). Our findings indicate that to take advantage of cDWI, the "saved time" attributable to the need for fewer images must be used to improve the SNR.

By applying present result to clinical case, cDWIs generated by adequate original images with arbitrary selected optimum *b*-values may be able to improve tumor conspiquity of pale lesions lying in the noisy mammary glands, which are often seen in high *b*-value aDWIs. However, the cDWIs generated form original images with insufficient SNR may easily cause inferior conspiquity to aDWIs, because tumor-background mammary gland contrast of cDWI does not exceed beyond that of the source images.

Paradoxically, the SNR and CNR of single *b*-value cDWI series obtained at NEX = 4 were higher than on images acquired at NEX = 8 (Fig. 6b and 6d). We speculate that, when the NEX is increased, the signal additions are performed at the real images level rather than the *k*-space level to avoid losing the randomness of phase information. Theoretically, the SD of the ROI does not decrease when the NEX is increased.[20]

In present study, the strength of the magnetic field of the clinical research and the phantom experiment was different due to equipment renewal during the research period. However, there is a report that DWI signal attenuation and ADC do not depend on equipment and magnetic field strength.[21] Therefore, this research is applicable regardless of the magnetic field strength, *b*-values, or vendor.

Our study has some limitations. In the phantom study we used a single bi-exponential decay phantom mimicking

the signal decay observed on breast tumor images. We recognize that our findings cannot be extrapolated to all patients. We think that the advantage of cDWI will be increased when tumor signal attenuation resembles mono-exponential decay. Studies investigating tumor conspicuity on phantom images with different multi-exponential decay patterns are needed.

In our clinical study we did not compare the sensitivity and specificity for breast tumor detection of multi-*b*-value aDWI and cDWI scans computed directly from high-SNR source images. Future studies must be performed to determine whether the diagnostic performance of high SNR cDWI exceeds that of multi-*b*-value aDWI.

Conclusion

In conclusion, to improve the conspicuity of breast tumors on cDWIs, the SNR of the source images must be improved. cDWI is possible to create high SNR, high *b*-value DWIs of the breast. However, with respect to the visualization of breast tumors, cDWI generated with the same imaging parameters as conventional measured high *b*-value DWIs did not yield superior results. It is important to recognize that the contrast on high *b*-value cDWIs is inferior to the contrast on aDWIs and that breast tumors may disappear on high *b*-value cDWIs.

Conflicts of Interest

The authors declare that they have no conflicts of interest.

References

1. Woodhams R, Matsunaga K, Iwabuchi K, et al. Diffusion-weighted imaging of malignant breast tumors: the usefulness of apparent diffusion coefficient (ADC) value and ADC map for the detection of malignant breast tumors and evaluation of cancer extension. J Comput Assist Tomogr 2005; 29:644–649.
2. Sinha S, Lucas-Quesada FA, Sinha U, DeBruhl N, Bassett LW. In vivo diffusion-weighted MRI of the breast: potential for lesion characterization. J Magn Reson Imaging 2002; 15:693–704.
3. Sharma U, Danishad KK, Seenu V, Jagannathan NR. Longitudinal study of the assessment by MRI and diffusion-weighted imaging of tumor response in patients with locally advanced breast cancer undergoing neoadjuvant chemotherapy. NMR Biomed 2009; 22:104–113.
4. Pereira FP, Martins G, Figueiredo E, et al. Assessment breast lesions with diffusion-weighted MRI: comparing the use of different *b* values. AJR Am J Roentgenol 2009; 193:1030–1035.
5. Bogner W, Gruber S, Pinker K, et al. Diffusion-weighted MR for differentiation of breast lesions at 3.0 T: how does selection of diffusion protocols affect diagnosis? Radiology 2009; 253:341–351.
6. Guo Y, Cai YQ, Cai ZL, et al. Differentiation of clinically benign and malignant breast lesions using diffusion-weighted imaging. J Magn Reson Imaging 2002; 16:172–178.
7. Peters NH, Borel Rinkes IH, Zuithoff NP, Mali WP, Moons KG, Peeters PH. Meta-analysis of MR imaging in the diagnosis of breast lesions. Radiology 2008; 246:116–124.
8. Koh DM, Collins DJ. Diffusion-weighted MRI in the body: applications and challenges in oncology. AJR Am J Roentgenol 2007; 188:1622–1635.
9. Charles-Edwards EM, de Souza NM. Diffusion-weighted magnetic resonance imaging and its application to cancer. Cancer Imaging 2006; 6:135–143.
10. Ochi M, Kuroiwa T, Sunami S, et al. Diffusion-weighted imaging (*b* value = 1500 s/mm^2) is useful to decrease false-positive breast cancer cases due to fibrocystic changes. Breast Cancer 2013; 20:137–144.
11. Woodhams R, Kakita S, Hata H, et al. Diffusion-weighted imaging of mucinous carcinoma of the breast: evaluation of apparent diffusion coefficient and signal intensity in correlation with histologic findings. AJR Am J Roentgenol 2009; 193:260–266.
12. Takanaga M, Hayashi N, Miyati T, et al. [Influence of *b* value on the measurement of contrast and apparent diffusion coefficient in 3.0 Tesla breast magnetic resonance imaging]. Japan J Radio Technol 2012; 68:201–208. (in Japanese)
13. Tamura T, Murakami S, Naito K, Yamada T, Fujimoto T, Kikkawa T. Investigation of the optimal *b*-value to detect breast tumors with diffusion weighted imaging by 1.5-T MRI. Cancer Imaging 2014; 14:11.
14. Yoshida R, Yoshizako T, Katsube T, Tamaki Y, Ishikawa N, Kitagaki H. Computed diffusion-weighted imaging using 1.5-T magnetic resonance imaging for prostate cancer diagnosis. Clin Imaging 2017; 41:78–82.
15. Takeuchi M, Matsuzaki K, Harada M. Computed diffusion-weighted imaging for differentiating decidualized endometrioma from ovarian cancer. Eur J Radiol 2016; 85:1016–1019.
16. Moribata Y, Kido A, Fujimoto K, et al. Feasibility of computed diffusion weighted imaging and optimization of *b*-value in cervical cancer. Magn Reson Med Sci 2017; 16:66–72.
17. Blackledge MD, Leach MO, Collins DJ, Koh DM. Computed diffusion-weighted MR imaging may improve tumor detection. Radiology 2011; 261:573–581.
18. O'Flynn EA, Blackledge M, Collins D, et al. Evaluating the diagnostic sensitivity of computed diffusion-weighted MR imaging in the detection of breast cancer. J Magn Reson Imaging 2016; 44:130–137.
19. Tamura T, Usui S, Murakami S, et al. Biexponential signal attenuation analysis of diffusion-weighted imaging of breast. Magn Reson Med Sci 2010; 9:195–207.
20. Ozaki M, Ogura A, Muro I, et al. [Influence of imaging parameters on the measurement of apparent diffusion coefficient]. Japan J Radio Technol 2010; 66:1178–1185. (in Japanese)
21. Ogura A, Tamura T, Ozaki M, et al. Apparent diffusion coefficient value is not dependent on magnetic resonance systems and field strength under fixed imaging parameters in brain. J Comput Assist Tomogr 2015; 39:760–765.